

White lines at K edges of light atoms

C. R. Bradley, M. L. Wroge, A. K. Dozier, and P. C. Gibbons
Department of Physics, Washington University, St. Louis, Missouri 63130
 (Received 2 August 1984)

Al, Si, and Mg in various solids have broad, prominent peaks at the thresholds of their K -shell ionization spectra. X-ray and electron-energy-loss data are in good agreement. Present theories of atoms and of solids, including some many-electron theories, do not explain these features.

I. INTRODUCTION

White lines in x-ray absorption spectra are prominent peaks at core-excitation thresholds. The name comes from their appearance in photographically recorded data. In all cases in which they are understood, they are caused by transitions from the core state to one or more localized, excited states. The classic example is the K -shell spectrum of argon gas, measured and analyzed by Parratt.¹ A Rydberg series with hydrogenic spacing but modified oscillator strengths, followed by a threshold and a smooth continuum, all broadened a bit, match the data well. In the overlapping, bound final states, the continuum threshold cannot be found without a detailed analysis of the spectrum.

Fano² discussed spectra of less-deeply bound shells in heavier atoms and in molecules. Drawing on his experience with inner wells in atomic potentials,³ he proposed that the strong white lines in core-excitation spectra of central atoms in molecules might be caused by excited states localized within the molecule, but not confined to the central atom. Measurements and calculations performed by Kutzler, Hodgson, Misemer, and Doniach⁴ have confirmed this idea. In complicated molecules containing ErCl_3 clusters, they obtained agreement between theory and experiment comparable to Parratt's in Ar.

White lines appear in solids too. In d -band metals, Brown, Peierls, and Stern⁵ show evidence that transitions to the partially filled d -shell cause them. Even though these materials are conductors, they have the localized, excited states that appear to cause all white lines. In the semiconductors Ge and Se, Brown, Peierls, and Stern show white lines at the K -excitation thresholds. They write that they are caused by excitons, without further elaboration. Grunes also finds⁶ that his spectra, from oxides of transition metals that have d bands at least half-filled, are strongly affected by the exciton interaction.

White lines in semiconductors may be core excitons. If so, they differ from the mobile, electron-hole pairs with excitation energies near the fundamental gap energy, in two ways. First, in a core exciton the hole is localized on a single atom.⁷ The electron in the core exciton stays near the unmoving ion. Second, the white lines have an intrinsic width of a few eV, more than the energy gap in the materials. They must be, not bound states below the lowest conduction-band energy, but more like atomic resonances in the continuum of conduction states.

II. EXPERIMENT

Electron-energy-loss spectroscopy provides data with good signal-to-noise ratios, for excitation energies up to 3 keV. Forward scattering produces energy-loss spectra that are simply related to optical-absorption spectra. The relation is

$$\sigma(E) = \pi^2 \alpha a_0^2 q^2 E \left. \frac{d\sigma}{d\Omega dE} \right|_{q=E/c}, \quad (1)$$

where σ is the optical-absorption cross section at frequency E/h and the differential cross section for electron scattering on the right-hand side is evaluated for energy transfer E and for momentum transfer, q , equal to the photon momentum. The constants α and a_0 are the fine-structure constant and the Bohr radius, respectively. As the scattering angle increases, the momentum transfer also increases, and nondipolar transitions begin to appear in the energy-loss spectra.

Electron-scattering data contain multiple-scattering contributions as well as the desired, single-scattering information. Single-scattering, core-excitation spectra can be extracted from measured data by a simple deconvolution.⁸ The method used approximates a deconvolution in three dimensions, such as that of Batson.⁹ The procedure described by Leapman and Swyt¹⁰ that simplifies the task for core-excitation data has been incorporated. The deconvolution was performed by successive operations of convolution and subtraction, rather than by Fourier transformation. Three-dimensional integrals over energy loss and transverse momentum transfer were reduced by analytic approximations to one-dimensional integrals over energy loss, with energy-dependent factors in the integrand that depend on the momentum-transfer acceptances used in gathering the data. The method is accurate for samples with uniform thickness. For a wedge of material, the method underestimates the true correction; what is subtracted from the data is not as large as it should be, although it is within a factor of 2 of what it should be.

In all figures in this paper, a smooth background has been subtracted, to leave only the contributions to the spectra from core excitations. After subtracting the measured dark counting rate from the data, typically a few counts from a few times 10^4 , the background was fitted over a range of energies below the threshold. The fitting

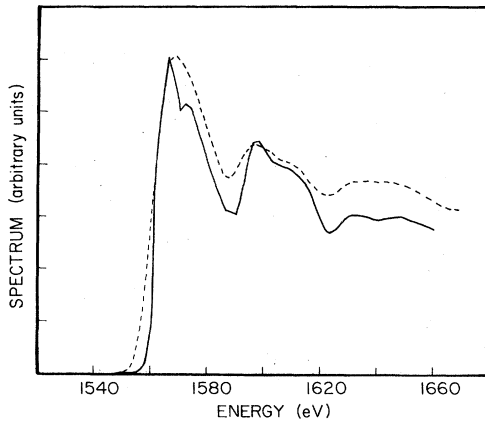


FIG. 1. *K*-shell excitation spectra of polycrystalline aluminum. The dashed curve is an electron-energy-loss spectrum measured in the forward-scattering direction. The solid curve is an x-ray absorption spectrum reported in Ref. 12.

function was AE^{-m} , where A and m were to be determined and E was the energy loss. The value of m varied from 2.5 to 4 between data sets, but varied by only a few percent for fitting ranges from 20 eV to 200 eV in the same data set. A chi-squared test indicated that the fits were as good as could be expected and that counting statistics dominated the fluctuations in the data.

The spectra in this paper were measured by electron scattering¹¹ unless a caption states otherwise, and multiple scattering has been removed from the energy-loss spectra if the caption does not state that it is there. All measured spectra shown in the same figure have been scaled to have equal maxima, because absolute calibrations were not made. Calculated spectra are presented as cross sections per atom, with units shown. Signals in the experiment were typically 10^5 counts above the background, per channel. The energy-loss spectra presented here are all broadened by an instrumental resolution of about 8 eV full width at half maximum (FWHM). The energy of the

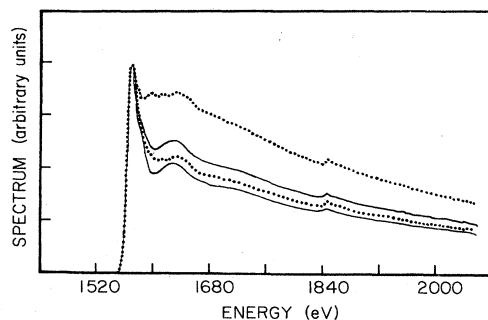


FIG. 2. *K*-shell excitation spectra of Al in oxidized films. The upper, dotted curve is from a sample thicker than usual. The lower, dotted curve is from a very thin sample. Both show the data before deconvolution. The upper, solid line is the spectrum of the thicker sample after a deconvolution to remove multiple scattering. The lower, solid spectrum is the same from the thin sample. The feature near 1840 eV is probably Si contamination.

primary beam was 79 keV. The longitudinal momentum transfer, fixed by kinematics, was about 1.6 \AA^{-1} . Transverse momenta were accepted in a range with a radius of approximately 2 \AA^{-1} centered on the forward-scattering direction. This corresponds to an angular resolution of 0.028 rad, full width. The samples produced by evaporation were between 200 and 400 Å thick.

Figure 1 shows the energy-loss and x-ray¹² spectra of aluminum metal. The energy resolution of the instruments that produced them is the only important difference between them. This demonstrates that the deconvolution works. To prove it again, Fig. 2 shows spectra from oxidized¹³ samples of aluminum, one thicker than usual and one very thin. They are different before deconvolution, the same after. Deconvolution yields almost the same spectra as do the occasional, very thin samples. Core-excitation spectra obtained by reducing energy-loss data are accurate, easily and quickly produced, and useful for studying features with energy widths of a few eV or more.

III. DATA AND COMMENTS

A. Data from solids

Figure 3 shows *K*-shell excitations of silicon in amorphous SiO_x , $1 \leq x \leq 2$, that was evaporated from SiO . Both this and the $\text{AlO}_x(\text{OH})_y$ in Fig. 2 have strong, broad white lines at threshold. The peak of the line is roughly twice as great as the mean level of the spectrum following it, in each case. The line is broader than the instrumental resolution in the oxidized aluminum, comparable in the oxidized silicon. In each case, near-edge structure and weak extended x-ray absorption fine structure (EXAFS) are present at energies above threshold.

The standard explanation, that white lines arise from strong transitions to localized final states, remains a good starting point for understanding the data in Figs. 2 and 3. Parratt's work¹ warns spectroscopists not to guess where continuum thresholds occur in their data. Nevertheless, the huge width of the threshold peak in the oxidized

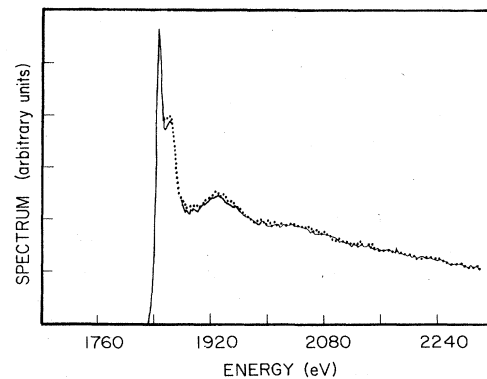


FIG. 3. *K*-shell excitation spectra of Si in films produced by evaporating silicon monoxide. The solid and dotted curves are from samples produced and measured at different times.

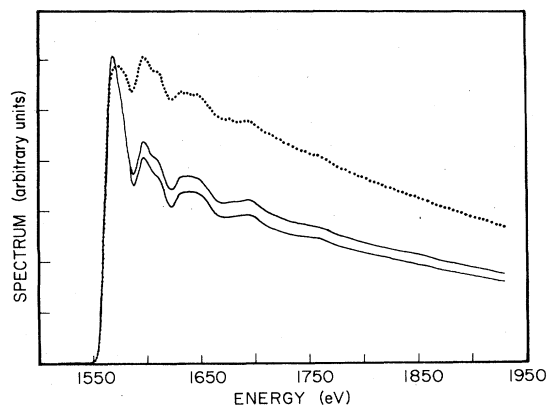


FIG. 4. *K*-shell excitation spectra of Al in a polycrystalline, metallic film. The dotted curve is the data before deconvolution. The lower spectra (solid curve) are the results of deconvolutions using two different measurements of the scattering at lower energies.

aluminum wrecks any explanation that involves only localized final states. The valence-conduction-band gap in the material is not as great as this energy width. The standard explanation must expand to include the resonances in the continuum that are familiar in atomic physics.³ This is probably true for the oxidized silicon also. The white line, although narrow, includes some structure. This suggests that it is a composite feature, with an intrinsic width greater than the band gap in the material. Some of the localized final states must be transiently localized rather than truly bound to the site of the excitation.

The spectra of *K*-shell excitations from polycrystalline aluminum metal and from polycrystalline magnesium metal show strong white lines. Figure 4 shows the energy-loss data of Fig. 1 over a wider range of energy, and Fig. 5 shows data from magnesium. The prominence of the lines at threshold relative to the features at higher energies is clear. This is more difficult to understand. There are no one-electron states that are both above the bottom of the conduction band and localized on the positive ions in these metals. Conventional, many-body physics applied to metals does not find any resonances in the conduction band of the sort invoked above. Calculations

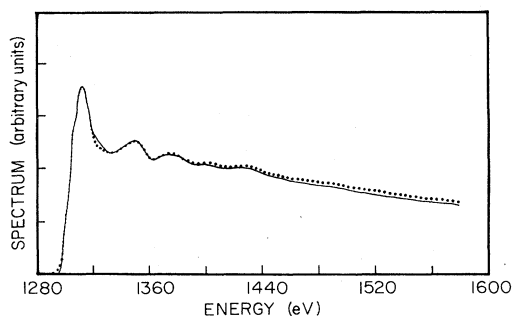


FIG. 5. *K*-shell excitation spectra of Mg in a polycrystalline, metallic film. The two spectra were gathered from different regions of the same sample.

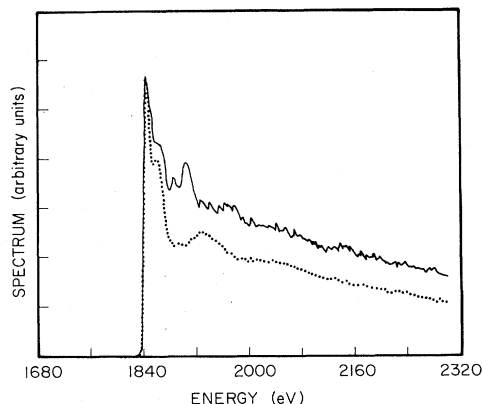


FIG. 6. *K*-shell excitation spectra of Si. The dotted curve is from a sample produced by evaporating silicon monoxide. The solid curve is from single-crystal Si that was thinned by chemical etching.

and measurements have shown that the Mahan–Nozières–de Dominicis (MND) effect is a small enhancement or suppression of a spectrum within a few tenths of an eV of the threshold.¹⁴ Calculations that go beyond the MND theory also produce spectra with only small enhancements above threshold.¹⁵ The sudden appearance of the core-hole potential in the conduction-electron system, which includes the excited electron, causes them. No calculation has produced features as strong as those shown in Figs. 4 and 5.

It is interesting to compare the spectra from metallic and oxidized samples of aluminum, and likewise from single crystal and oxidized silicon. Figure 6 shows the comparison for silicon, Fig. 7 for aluminum. The pure silicon sample was not uniform in thickness, so the data had to be gathered from an area only 1 μm in diameter. This kept the range of thickness sampled sufficiently small that the removal of multiple scattering should be accurate, at least to within the noise in the result. That noise is large because the signal from the small area was smaller than usual. Any variation of the thickness over the area from which the data were gathered would make the white line in the Si crystal even stronger, relative to the spectrum at higher energies above threshold, than what is shown in

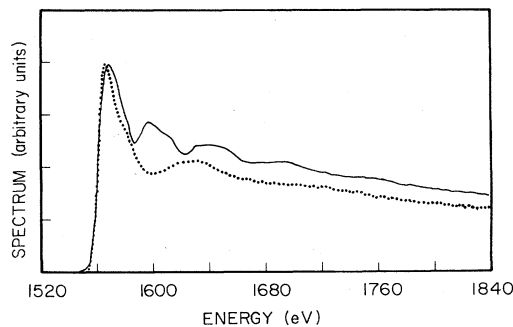


FIG. 7. *K*-shell excitation spectra of Al. The solid curve is from a polycrystalline, metallic film. The dotted curve is from an oxidizing film.

Fig. 6. The white line is similar to the one from oxidized silicon, and also similar to the one from SiN observed by Leapman and Swyt.¹⁰ In the aluminum, the white lines in the metal and in the oxide are clearly the same. The near-edge structure and EXAFS at higher energies are different in the two materials, but not the threshold peak. This reduces the range of acceptable explanations.

B. Vapor-phase data

K-shell excitation spectra have been published for Na¹⁶ and for Ar.¹⁷ Both display rich structure, much sharper in energy than any spectra shown here. Most of the peaks are confidently assigned to single configurations with either one or two excited electrons. Neither spectrum has a broad, white line like the ones shown in this paper, not even if the resolution is reduced by broadening the data. Manson¹⁸ has pointed to a feature in the Ar spectrum that is a many-electron effect in the excitations to the continuum. It is an enhancement of the oscillator strength within a few tens of an eV above threshold, but it is much weaker than the white lines presented here.

IV. CALCULATIONS

A simple calculation provides useful insight into the present problem. It estimates atomic, K-shell, excitation spectra by calculating a transition matrix element in the one-electron approximation. The initial state is a Clementi-Roetti 1s wave function.¹⁹ The final state is a free wave, obtained by integrating the radial part of the one-electron Schrödinger equation with a potential that is computed using the Clementi-Roetti wave functions for the occupied orbitals. Exchange and correlation are included using the local-density approximation.²⁰⁻²² The results are different from the hydrogenic approximation,^{23,24} in which eigenstates of a Coulomb potential with an effective charge near that of the nucleus are used. Figure 8 shows results for Mg. The effect of the core-hole potential on the spectrum has been estimated by using optical alchemy;²⁵ the $Z + 1$ ion approximation.²² The exciton interaction between the excited electron and the positive charged ion has two effects here. First, it reduces the oscillator strength over the entire range shown in Fig. 8.

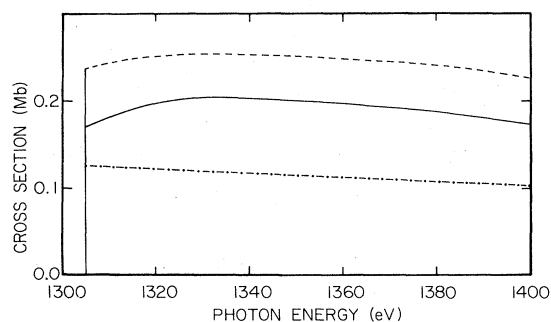


FIG. 8. Optical-absorption cross section of the K shell of an Mg atom. The dashed spectrum does not include the effect of the core-hole potential. The solid curve does. The calculation is described in the text. The dot-dashed curve is the hydrogenic approximation of the spectrum.

Second, it slightly enhances the peak 25 eV above threshold relative to the rest of the spectrum. The hydrogenic approximation gets only half of the better estimate of the strength.

In this model, the core-hole potential does not produce a white line. The redistribution of oscillator strength it produces is a smooth function of energy, much smaller than the average strength. The model does not include any bound, unoccupied, atomic states, but there should be none in the metallic Mg measured here. A local-field calculation²⁰ that is equivalent to the random-phase approximation in an atom produces identical spectra. In these light atoms, electron correlations beyond Hartree-Fock with Slater exchange are not important.

The most interesting feature of the data is the similarity of the white lines in metallic and oxidized Al. The line in the metal is especially difficult to understand. All the excited states should be extended there, even if the effective potential of the core-hole is included. Bryant and Mahan have a calculable model for excitations of an atom in a metal.²¹ It is a jellium with a spherical void in which one atom is placed. They calculate a one-electron transition rate, in an effective potential that represents both the atom and the metallic screening accurately. Figure 9 shows the results that Mehl *et al.* obtained²⁶ for the 1s spectrum of Al. The calculation was done both with and without the added, effective potential of the core hole. Its effect is to move oscillator strength down in energy, toward the threshold. It produces a peak just above threshold, but one much weaker than the white lines in the data.

Band-structure calculations give accurate one-electron wave functions that can be used to calculate transition rates. They always leave out the core-hole potential. The *p*-wave projection of the density of states in aluminum metal has been calculated by Smulowicz and Segall²⁷ to 22 eV above the Fermi energy by the augmented-plane-wave (APW) method. The agreement of the fine details with higher-resolution experiments is good. Unfortunately, the energy range of the calculation is not great enough to tell whether band structure predicts the white line. Figure 10 shows the result, high-resolution data,²⁸ and the present data for comparison. Note that a band-structure explanation of one spectrum would open a new question: Why

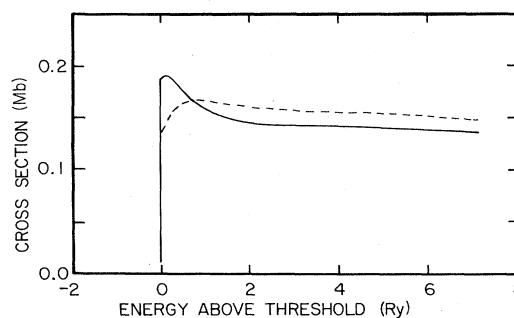


FIG. 9. Optical-absorption cross section calculated for the K shell of an Al atom in the metal. The solid curve was calculated including the potential of the core hole in the effective, one-electron potentials. The dashed curve was calculated without it. Mehl used the method described in Ref. 21 to calculate the spectra.

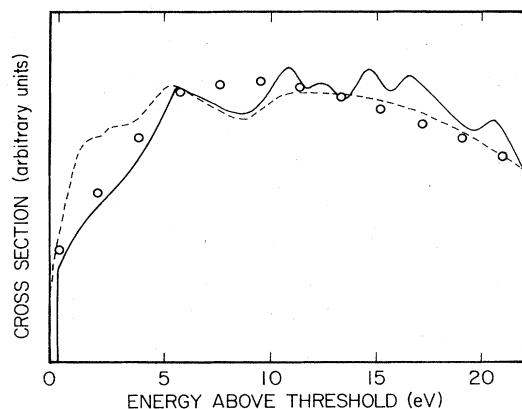


FIG. 10. Optical-absorption cross section for the K shell of an Al atom in the metal. The solid curve is a projected density of states from a band-structure calculation, Ref. 27. The dashed curve is x-ray data from Ref. 28. The points are energy-loss data from the present work.

should materials with different lattice structures and different energy gaps have the same feature in their densities of states above the Fermi energy?

V. CONCLUSIONS

The white line described here appears in the K -shell spectra of some elements in the Na-Ar row of the Periodic Table. It does not appear to be an atomic effect, first because it is not observed in the vapor-phase data that are

available, and second because calculations that should be accurate for these light atoms do not produce it. It does not appear to be a solid-state effect, because it is the same in a metal and a transparent insulator. A joint effect, such as resonance in the continuum somehow enhanced or sharpened by the presence of neighbor atoms at typical solid distances,² seems worth considering.

There is theoretical work that, if done, would remove some of the uncertainties. First, an APW calculation of the p -wave projection of the density of states in Al metal, extended from the Fermi energy to 100 eV above it, would show whether one white line has a simple explanation. It might well be extended to other materials. Second, and more difficult, is a band-structure calculation in a superlattice with one core hole in the center of each supercell, and something like 27 cells per supercell. This would show the effect of the core-hole potential in a good model of a solid. von Barth and Grossman have done such a calculation for Na, but only near the Fermi energy.²⁹ Salahub and Messmer³⁰ have done a molecular-cluster calculation for Al, but not with sufficient resolution or range to answer the question.

Experimental work is also needed. First, in electron-energy-loss spectroscopy, the spectra change shape as the momentum transfer increases. In many models it is possible to predict how this will occur. We are gathering and deconvoluting spectra over a range of momentum transfers to use the additional information. Second, to address the question of atomic versus solid-state effects, K -shell spectra of more of these elements in the vapor phase are needed.

¹Lyman G. Parratt, *Phys. Rev.* **56**, 295 (1939).

²U. Fano, *Comments on Atomic and Molecular Physics* (Gordon and Breach, New York, 1972), Vol. III, p. 75.

³U. Fano and J. W. Cooper, *Rev. Mod. Phys.* **40**, 441 (1968).

⁴Frank W. Kutzler, Keith O. Hodgson, D. K. Misemer, and S. Doniach, *Chem. Phys. Lett.* **92**, 626 (1982).

⁵M. Brown, R. E. Peierls, and E. A. Stern, *Phys. Rev. B* **15**, 738 (1977).

⁶L. A. Grunes, *Phys. Rev. B* **27**, 2111 (1983), and references therein.

⁷Harold P. Hjalmarson, Helmut Büttner, and John D. Dow, *Phys. Rev. B* **24**, 6010 (1981).

⁸C. R. Bradley, M. L. Wroge, and P. C. Gibbons, *Ultramicroscopy* (to be published).

⁹P. E. Batson, Ph.D. thesis, Cornell University, 1976.

¹⁰R. D. Leapman and C. R. Swyt, in *Analytical Electron Microscopy—1981*, edited by R. H. Geiss (San Francisco University Press, San Francisco, 1981), pp. 164–172.

¹¹Gatan, Inc., model no. 607 EELS spectrometer; Hitachi model no. HU 11B transmission electron microscope.

¹²Richard D. Deslattes, *Acta. Crystallogr. Sect. A* **25**, 89 (1969).

¹³Polycrystalline films of Al metal were oxidized by anodizing or by baking at 350°C for 1 h in the presence of steam.

¹⁴P. H. Citrin, G. K. Wertheim, and M. Schlüter, *Phys. Rev. B* **20**, 3067 (1979), and references therein.

¹⁵See, for example, G. D. Mahan, *Phys. Rev. B* **21**, 1421 (1980); U. von Barth and G. Grossman, *Phys. Scr.* **21**, 580 (1980); L. C. Davis and L. A. Feldkamp, *Phys. Rev. B* **23**, 4269 (1981).

¹⁶M. H. Tuilier, D. Laporte, and J. M. Esteve, *Phys. Rev. A* **26**, 372 (1982).

¹⁷R. D. Deslattes, R. E. LaVilla, P. L. Cowan, and A. Henins, *Phys. Rev. A* **27**, 923 (1983).

¹⁸S. T. Manson, in *X-Ray and Atomic Inner-Shell Physics—1982* (International Conference, University of Oregon), edited by Bernd Craseman (AIP, New York, 1982), p. 321.

¹⁹E. Clementi and C. Roetti, *At. Data Nucl. Data Tables* **14**, 177 (1974).

²⁰A. Zangwill and Paul Soven, *Phys. Rev. A* **21**, 1561 (1980).

²¹G. W. Bryant and G. D. Mahan, *Phys. Rev. B* **17**, 1744 (1978).

²²P. A. Lee and G. Beni, *Phys. Rev. B* **15**, 2862 (1977).

²³M. Inokuti, *Rev. Mod. Phys.* **43**, 297 (1971).

²⁴R. F. Egerton, *Ultramicroscopy* **4**, 169 (1979).

²⁵J. D. Dow, D. R. Franceschetti, P. C. Gibbons, and S. E. Schnatterly, *J. Phys. F* **5**, 1211 (1975).

²⁶G. W. Bryant (private communication); M. J. Mehl, T. L. Einstein, and G. W. Bryant (unpublished).

²⁷F. Szmulowicz and B. Segall, in *International Conference on the Physics of X-Ray Spectra* (National Bureau of Standards, Gaithersburg, Maryland, 1976), p. 202.

²⁸C. Senemaud and M. T. Costa Lima, *J. Phys. Chem. Solids* **37**, 83 (1976).

²⁹Ulf von Barth and Günter Grossman, *Solid State Commun.* **32**, 645 (1979).

³⁰D. R. Salahub and R. P. Messmer, *Phys. Rev. B* **16**, 2526 (1977).